# Reacting Flows in Industrial Duct-burners of a Heat Recovery Steam Generator

Petrone G.[1]*, Cammarata G.[1], Caggia S.[2], Anastasi M.[2]

[1] Department of Industrial and Mechanical Engineering, University of Catania
Viale Andrea Doria 6 – 95125 Catania, ITALY
[2] Engineering Maintenance - ISAB Energy Services
Priolo Gargallo (SR), ITALY

*Corresponding author: gpetrone@diim.unict.it

**Abstract:** In this study COMSOL Multiphysics is applied in order to simulate reacting flows for duct-burner systems arranged in the post-firing section of a Heat Recovery Steam Generator of a combined cycle power plant. Two- and three-dimensional simulations are carried-out in order to investigate on operative conditions mainly responsible of duct-burners overheating.

**Keywords:** combustion, reacting flow, heat transfer, industrial burners.

## 1. Introduction

A combined cycle power plant lay-out can be outlined as in following: gas turbines provide hot exhaust gases (Turbine Exhaust Gas, TEG) to a Heat Recovery Steam Generator (HRSG) producing working fluid for steam turbines. This technology assumes special advantages, from efficiency and environmental point of view, in the Integrated Gasification Combined Cycle plants (IGCC), where the power generation is assured by combustion of synthesis gas coming from gasification process of coal or petroleum distillation waste products. Concerning the HRSG, very often they are equipped by post-firing sections in order to produce very high temperature steam and also to balance losses in efficiency of the turbogas groups during the hotter season. The post-firing section very often consists in arrays of duct-burners mounted on horizontally arranged pipes providing fuel (Figure 1). TEG come from backside with respect to the post-firing section and supplying of fuel is assured by primary injection holes perpendicularly disposed with respect to the pipes axis. In the diffusion after-burner (Figure 2), the fuel is firstly injected into a recirculation chamber, bounded by front panels, and then into the combustion region, just to prevent backfiring, so mixing mainly occurs inside the flame.

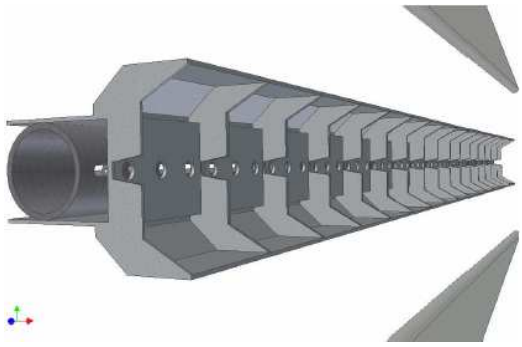

**Figure 1**. Three-dimensional model of a single duct-burner row.

Deflector wings and baffles drive the combustive fluid (TEG) in order to optimize matching with fuel flowing from the secondary injection hole of the recirculation chamber.

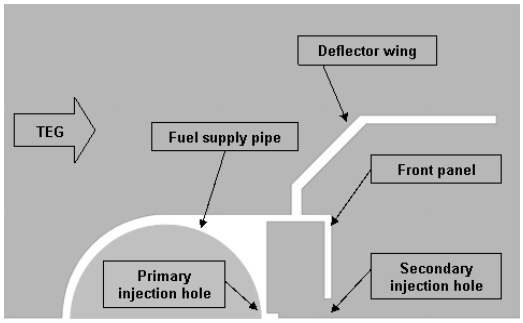


**Figure 2**. Two-dimensional outline of the studied diffusion duct-burner.

The duct-burners operative conditions are clearly affected by the TEG composition which modify stability range for combustion and also by the fuel's compounds: some gas impurities (Ni-carbonyl) becomes unstable at temperature above about 700 K (depending on concentration)

depositing metallic Ni on the burner contour. The deposit thickness enables cracking of the components. For that reason the burners must be cleaned to restore safe operating condition imposing expensive periodic plant stops. Also, a local excessive thermal level on the burner surface induces important mechanical stresses to those component. The present study is devoted to analyse witch operative conditions for the post-firing section could be responsible of regrettable temperature values on the burner's manifold.

## 2. Modelling

Modelling of the physical system is performed by exploiting COMSOL Multiphysics. At first a two dimensional model has been employed and then a three dimensional one; since the buoyancy forces is neglected, only a half of the symmetric geometrical system is analysed. Due to the complexity of the geometry, the physical domain is discretized by triangular or tetrahedral non uniform unstructured meshes (Figure 3).

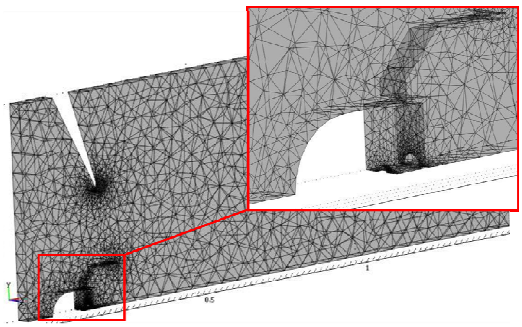

**Figure 3**. Numerical mesh for a 3D model and enlargement of the spatial region close to the inlet section for supplied fuel (recirculation chamber).

Since the tiny pressure variation, in order to reduce the computational effort, the flow is considered incompressible and the heat exchange between the gas and the after-burner body is also neglected. The turbulent flow in after-burner domain is solved by a k-ε method, that involves solution of the following equations:

$$\rho u \cdot \nabla u = \nabla \cdot \left[ -pI + (\eta + \eta_T)\left(\nabla u + (\nabla u)\right)^T \right] + F$$

$$\nabla \cdot u = 0$$

$$\rho u \cdot \nabla k = \nabla \left[ \left( \eta + \frac{\eta_T}{\sigma_k} \right) \nabla k \right] + \eta_T P(u) - \rho\varepsilon$$

$$\rho u \cdot \nabla \varepsilon = \nabla \left[ \left( \eta + \frac{\eta_T}{\sigma_\varepsilon} \right) \nabla \varepsilon \right] + \frac{C_{\varepsilon 1}\varepsilon \eta_T P(u)}{k} - \frac{C_{\varepsilon 2}\rho\varepsilon^2}{k}$$

where:

$$P(u) = \nabla u : \left(\nabla u + (\nabla u)^T\right) \text{ and } \eta_T = \frac{\rho C_\mu k^2}{\varepsilon}$$

The momentum equations are coupled with 5 transport-diffusion equations in order to solve concentration of reacting chemical species (CO, $H_2$, $O_2$, $CO_2$ and $H_2O$). The simplified chemical reaction for syngas oxidation is supposed to be:

$$CO + H_2 + O_2 \rightleftarrows H_2O + CO_2$$

The reference transport-diffusion equations are reported below:

$$\nabla \cdot \left(-D_{H_2} \nabla H_2\right) = R - u \cdot \nabla H_2$$
$$\nabla \cdot \left(-D_{CO} \nabla CO\right) = R - u \cdot \nabla CO$$
$$\nabla \cdot \left(-D_{O_2} \nabla O_2\right) = R - u \cdot \nabla O_2$$
$$\nabla \cdot \left(-D_{H_2O} \nabla H_2O\right) = R - u \cdot \nabla H_2O$$
$$\nabla \cdot \left(-D_{CO_2} \nabla CO_2\right) = R - u \cdot \nabla CO_2$$

Where the reaction rate R is defined as:

$$R = \pm\ k_1 \times O_2 \times H_2 \times CO \ \mp\ k_2 \times CO_2 \times H_2O$$

Since the exothermic nature of the reaction, thermal analysis is performed by considering a energy source, strictly related both to the reaction rate and the net reaction enthalpy for each one:

$$\nabla \cdot \left(-k \nabla T\right) = (R \times H) - \rho C_p u \cdot \nabla T$$

Where the net enthalpy of reaction is expressed as:

$$H = H_{CO_2} + H_{H_2O} - (H_{O_2} + H_{H_2} + H_{CO})$$

The numerical solving procedure for steady state solution lies on a iterative scheme based on a modified Newton-Raphson method for directly

solving the nonlinear system. Algebraic systems coming from differential operators discretization are solved by using a direct unsymmetrical multi-frontal method based on the LU decomposition. Computations have been carried-out on a 64 bit calculator disposing of 16 GB of RAM.

## 3. Results

The results are obtained for several chemical compositions of the supplied fuel (0.815 to 1.04 referring to the H2/CO value and LHV swings around 13.5 MJ/kg), that consists in a typical standard gasification petrol by product. Effect of thermal load is also analysed (0.8÷1.2 MWth/m), referring to possible turn-down operating condition in power plant applications. From results appears that fuel composition does not affect sensibly after-burners functioning conditions On the other hand, simulations well highlight as modification in fluid-dynamical distribution, related to increasing in mass flow rate of reactants, seriously compromise flame stability.

### 3.1 Specific thermal power 0.8 MWth/m

Figure 4 shows an enlargement of the velocity field and the streamlines of flow obtained for 0.8 MWth/m of specific power supplied by the post-firing section.

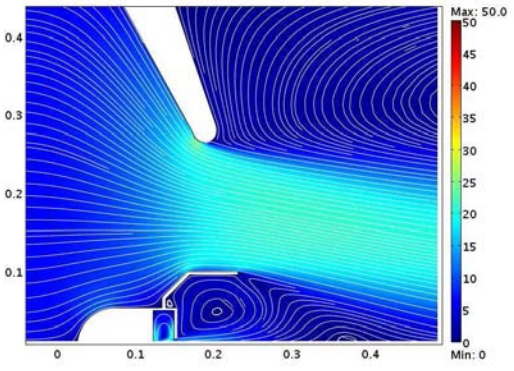


**Figure 4.** Velocity field and streamlines of flow obtained for 0.8 MWth/m.

In that figure the vein contraction due to the effect of the baffle and the deflector wing is clearly observable. Those elements drive the TEG to the fuel jet, in order to assure a correct mixing by flows diffusion. The fuel inlet generates a first anti-clockwise vortex inside the chamber, that is operationally exploited in order to cool the burner manifold. Then the fuel coming out from the secondary injection hole generates a second anti-clockwise cell adjacently to the external surface of the front panel. From a chemical point of view, flows mixing and reaction is well evidenced by illustration of Figure 5, where $CO_2$ molar fraction distribution is reported.

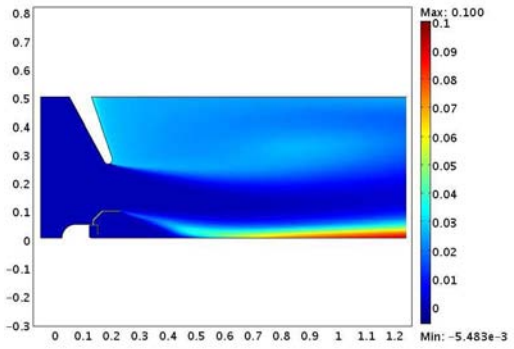


**Figure 5**. Molar fraction of $CO_2$ obtained for 0.8 MWth/m.

The flame anchorage at the deflector wing is also highlights by Figure 6 that shows the thermal field obtained for the above mentioned specific thermal power supplied by the post-firing section of the HRSG.

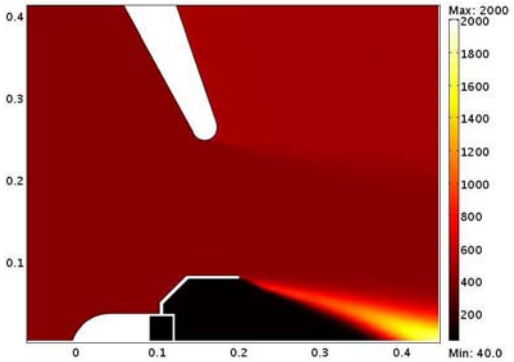


**Figure 6.** Thermal field obtained for 0.8 MWth/m.

By looking at that picture it is to notice as, during 0.8 MWth/m power supplying condition, temperature close to the burner manifold does

not reach values compatible with metal deposition of Nichel compounds on the front panel surface (the threshold value is around 700 K).

### 3.2 Specific thermal power 1.2 MWth/m

This load condition characterises the so called turn-down operational condition. Figure 7 presents velocity field and streamlines of flow obtained by increasing the mass flow rates of reactants in order to assure the above mentioned specific power. From comparison with Figure 4 it is to observe as a new small clockwise vortex stands in correspondence of the deflector wing extremity. This fluid roll partially allows TEG to U-turn and so flow very close to second injection hole of the burner. This fluid-dynamic modification is seen to have very important effects. In fact that circulation allow the fluids to meet each other and react close to the front panel surfaces, as illustrated by picture reported in Figure 8 where the molar fraction of $CO_2$ is drawn for the actually analysed thermal load. As a consequence, temperature field, reported in Figure 9, results really modified with respect with that one computed for the lower specific power, previously discussed.

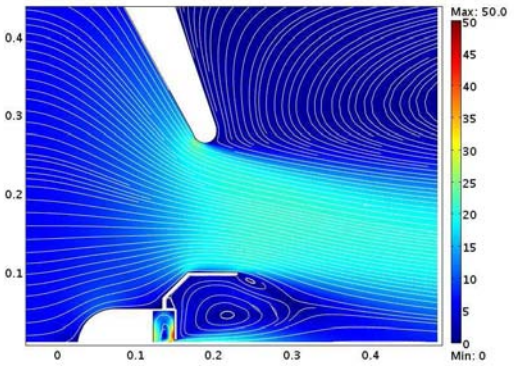


**Figure 7**. Velocity field and streamlines of flow obtained for 1.2 MWth/m.

This time thermal field representation highlights a critical state for the burner front section, due to the very high temperature of the flame occurring just adjacent to it. Flame triggering during "turn-down condition" results too close to after-burners manifold, so that high thermal stresses could be produced. Convective effects on thermal distribution are also well appreciable by looking Figures 7 and 9 together.

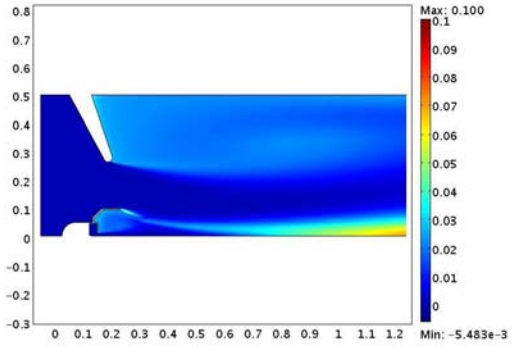


**Figure 8**. Molar fraction of $CO_2$ obtained for 1.2 MWth/m.

From the performed analyses it is possible to affirm that increasing in mass flow rates of reactants, in order to supply higher thermal load at the post-firing section, could be considered as one of the critical operative condition with respect to overheating of the burners manifold. The previously showed results have also been confirmed by 3D simulations.

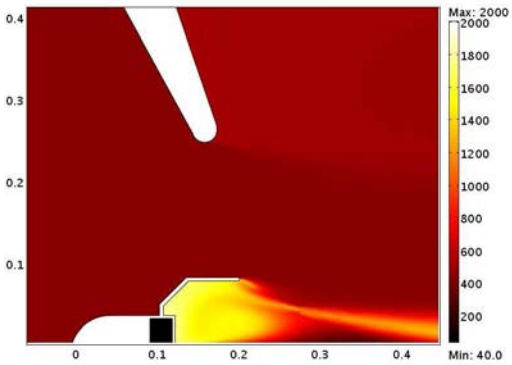


**Figure 9**. Thermal field obtained for 1.2 MWth/m.

For those simulations it has been taken into consideration a model reproducing a portion of one module of the duct-burners (each module disposes of three holes for fuel injection, see Figure 1). Figure 10 and 11 report velocity field, streamlines of flow and isothermal surfaces for a simulation done at specific thermal load of 1.2 MWth per meter of duct-burner length. The occurrence of the small clockwise fluid roll anchored to the deflector wing is less evident

with respect to 2D representation. This is mainly imputable to the quite hardness in post-processing and visualization for 3D numerical results. In spite of this, thermal representation well highlights as combustion happens too much close to the burner manifold.

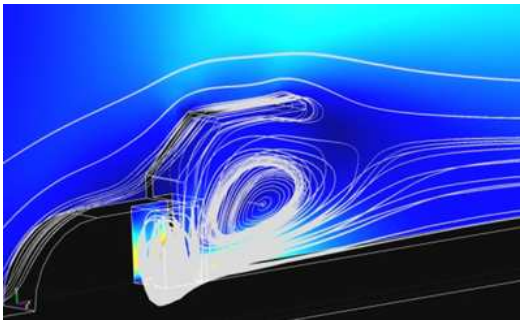

**Figure 10**. Velocity distribution and streamlines of flow for 3D simulation.

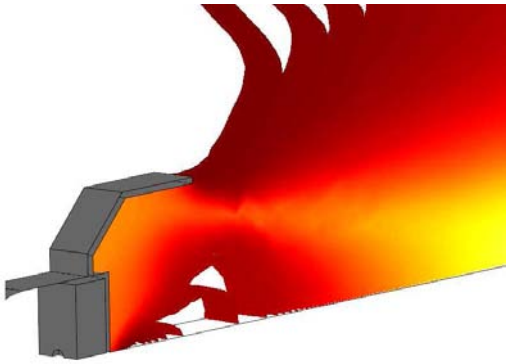

**Figure 11**. Isothermal surfaces for 3D simulation.

### 3.3 Brisk combustion due to TEG leakages

The onset of a dangerous brisk combustion, related to TEG leakages through out the assembled array of duct-burners, has been also detected by 3D simulations. During burner's array assembling all the modules are not well fitted each other so a little slight gap has been noticed during inspection. Examine Figures 12, the hot TEG's leakage inside the recirculation chamber could lead to a brisk combustion that heats up to melting the burner body. In order to assess the previous considerations some simulations have been done by considering a geometrical model reproducing the occurrence of a tiny slot between the burner manifold and the numerical confinement (lateral wall of the domain). This model is representative of one half of the upper half portion of one module. Results of simulations confirmed the potential brisk combustion related with the previously mentioned geometrical slot between adjacent modules.

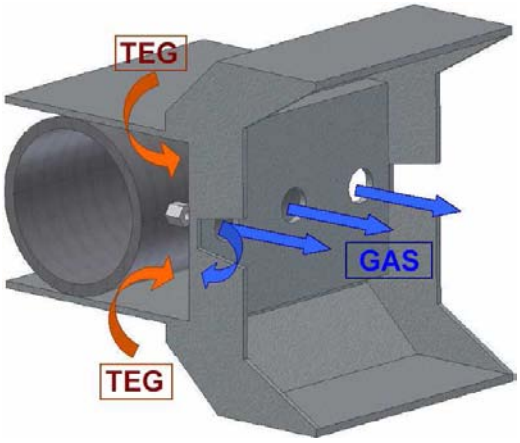


**Figure 12**. Outline of the TEG leakage through out the gap between adjacent after-burners.

As clearly illustrated by Figures 13, where molar fraction are reported for $O_2$ (left side of Figure 13) and $H_2$ (right side of Figure 13), it exists the opportunity that oxidising and fuel compounds meet each other inside the recirculation chamber.

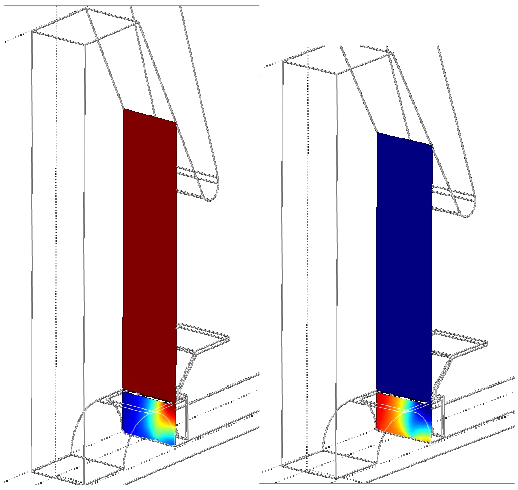

**Figure 13**. Molar fraction of $O_2$ (right side) and $H_2$ (left side) on a transversal section.

The occurrence of the brisk combustion in proximity of the recirculation chamber is well evidenced by looking at Figure 14, where molar fraction of $CO_2$ is reported on two longitudinal sections of the numerical model. From the analysis of Figure 14 it is possible to summarize that products reaction concentration, standing inside the recirculation chamber, highly increases if section is considered in proximity of the duct-burners module lateral end.

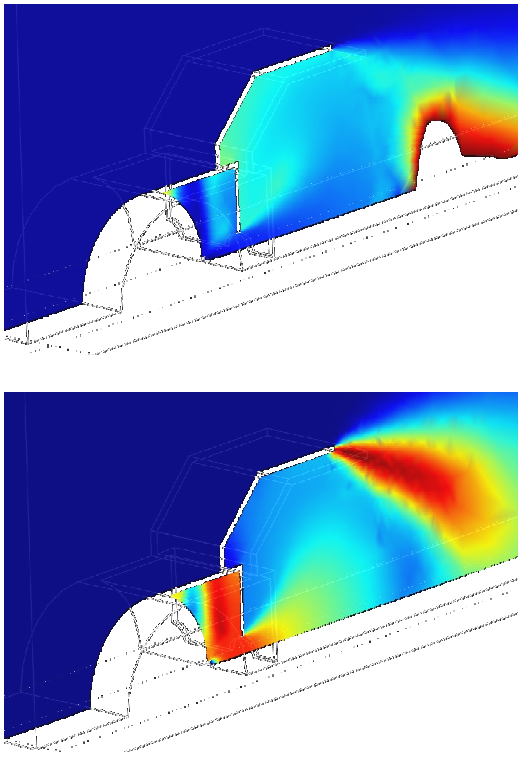

**Figure 14**. Molar fraction of $CO_2$ on consecutive longitudinal sections.

## 4. Conclusions

In this study the FEM based software COMSOL Multiphysics is applied in order to simulate reacting flows for duct-burner systems arranged in the Heat Recovery Steam Generator of a combined cycle power plant. Fluid-dynamical analysis is performed exploiting a k-ε turbulence method, while 5 transport-diffusion equations are solved in order to simulate the reacting flow of CO, $H_2$, $O_2$, $CO_2$ and $H_2O$, respectively. Reaction enthalpy is considered as source term in the energy balance in order to solve thermal field of the computational domains. The results are obtained for several chemical compositions of the supplied fuel and for several values of the fuel mass flow rate incoming inside the control volume. Some operative conditions concerning mass flow rate of fuel are seen to determinate regrettable high temperature values on the after-burners manifold. Three-dimensional simulations principally show as an accurate design of the combustors array is strictly needed in order to assure a wide-stable operating condition range. The present work clearly shows as the numerical approach represents a powerful tool of investigation for this kind of industrial applications.

## 5. References


1. S. Ahmed, J.Hart, J. Nikolov, C. Solnordal, W. Yang, J. Naser, The effect of a jet velocity ratio on aerodynamics of cross-flow, *Experimental Thermal and Fluid Science*, Vol. 32 (2007), pp. 362–374.

2. C.K. Westbrook, Y. Mizobuchi, T. J. Poinsot, P. J. Smith, J. Warnatz, Computational combustion, *Proceedings of the Combustion Institute*, Vol. 30 (2005), pp. 125–157.

3. M. Modesto, S.A. Nebra, Analysis of a repowering proposal to the power generation system of a steel mill plant through the exergetic cost method, *Energy*, Vol. 31 (2006), pp. 3261–3277.

4. L. A. Catalano, A. Dadone, D. Manodoro, A. Saponaro, Thermal design and emissions of duct-burners for combined-cycle and cogenerative plants, *International Journal of Environmental Technology and Management*, Vol. 23 (2005), pp. 108-119.

5. K.H. Yong, Method of gasification in IGCC system, International *Journal of Hydrogen Energy*, Vol. 32 (2007), pp. 5088-5093.

6. K.-T. Wu, H.T. Lee, C.I. Juch, H.P. Wan, H.S. Shim, B.R. Adams, S.L. Chen, Study of syngas

co-firing and reburning in a coal fired boiler, *Fuel*, Vol. 83 (2004), pp. 1991–2000.

7. A. Cuoci, A. Frassoldati, G. Buzzi Ferraris, T. Faravelli, E. Ranzi, The ignition, combustion and flame structure of carbon monoxide/hydrogen mixtures. Note 2: Fluid dynamics and kinetic aspects of syngas combustion, *International Journal of Hydrogen Energy*, Vol. 32 (2007), pp. 3486-3500.

8. F.H.V. Coppens, J. De Ruyck, A.A. Konnov, The effects of composition on burning velocity and nitric oxide formation in laminar premixed flames of CH4 + H2 + O2 + N2, *Combustion and Flame*, Vol. 149 (2007), pp. 409–417.

9. A.X. Sengissen, J.F. Van Kampen, R.A. Huls, G.G.M. Stoffels, J.B.W. Kok, T.J. Poinsot, LES and experimental studies of cold and reacting flow in a swirled partially premixed burner with and without fuel modulation, *Combustion and Flame*, Vol. 150 (2007), pp. 40–53.

10. ISAB Energy Services, Inspection Book 2005, Priolo Gargallo (I), (2005).

11. ISAB Energy Services, Inspection Book 2007, Priolo Gargallo (I), (2007).

## 6. Acknowledgements

The authors thanks for its precious contribution Eng. L. Nobile of the Engineering Maintenance of the ISAB Energy Services (Priolo Gargallo (SR), Italy). Sincere words of thanks are due to Eng. A. Saponaro, Head of the Combustion and Environment Centre (Gioia del Colle (BA), Italy).